

PAPER • OPEN ACCESS

Biphasic epoxy-ionic liquid structural electrolytes: minimising feature size through cure cycle and multifunctional block-copolymer addition

To cite this article: Quan Wendong *et al* 2021 *Multifunct. Mater.* 4 035003

View the [article online](#) for updates and enhancements.



ECS The Electrochemical Society
Advancing solid state & electrochemical science & technology
2021 Virtual Education

Intensive Short Courses

Sunday, October 10 & Monday, October 11

Providing students and professionals with in-depth education on a wide range of topics

[CLICK HERE TO REGISTER](#)

Multifunctional Materials



PAPER

OPEN ACCESS

RECEIVED
13 April 2021

REVISED
6 August 2021

ACCEPTED FOR PUBLICATION
18 August 2021

PUBLISHED
9 September 2021

Original content from this work may be used under the terms of the [Creative Commons Attribution 4.0 licence](https://creativecommons.org/licenses/by/4.0/).

Any further distribution of this work must maintain attribution to the author(s) and the title of the work, journal citation and DOI.



Biphasic epoxy-ionic liquid structural electrolytes: minimising feature size through cure cycle and multifunctional block-copolymer addition

Quan Wendong¹, John Dent¹, Valeria Arrighi², Leide Cavalcanti³, Milo S P Shaffer⁴ and Natasha Shirshova^{1,*} 

¹ Department of Engineering, Durham University, South Road, Durham DH1 3LE, United Kingdom

² School of Engineering and Physical Sciences, Institute of Chemical Sciences, Heriot-Watt University, Edinburgh EH14 4AS, United Kingdom

³ Science Technology Facilities Council, Isis Neutron and Muon Source, Harwell Campus, Oxfordshire OX11 0QX, United Kingdom

⁴ Department of Materials, Imperial College London, South Kensington Campus, London SW7 2AZ, United Kingdom

* Author to whom any correspondence should be addressed.

E-mail: natasha.shirshova@durham.ac.uk

Keywords: structural electrolyte, bicontinuous structure, reaction induced phase separation, block-copolymer, epoxy resin, ionic liquid

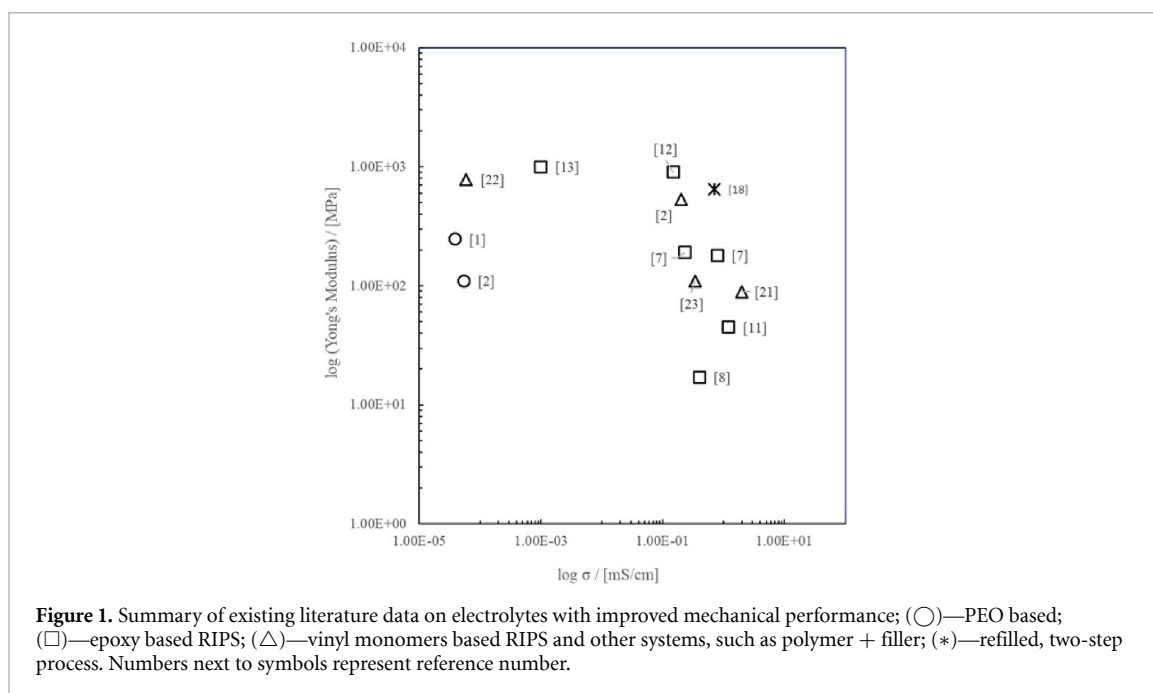
Supplementary material for this article is available [online](#)

Abstract

Structural electrolytes provide mechanical properties approaching structural resin combined with a high degree of ionic conductivity. Here, structural electrolytes based on bisphenol A diglycidyl ether and the ionic liquid 1-ethyl-3-methylimidazolium bis(trifluoromethylsulfonyl) imide (EMIM-TFSI) were synthesised through reaction induced phase separation (RIPS) using isophorone diamine (iPDA) as a curing agent. The microstructure and properties of the resulting materials were controlled through both the initial formulations and the curing temperature. Curing at room temperature generated a bi-continuous structure and improved both mechanical performance and ionic conductivity of the resulting structural electrolytes. The balance between properties can be systematically adjusted; for example, a promising Young's modulus of 800 MPa was obtained simultaneously with an ionic conductivity of 0.28 mS cm^{-1} , for a formulation containing 35 vol% EMIM-TFSI. The lengthscale of the structural features was reduced by an order of magnitude by introducing multifunctional block-copolymers (MF-bcP) based on glycidyl methacrylate (GMA) and quaternised (2-dimethylamino)ethyl methacrylate (DMAEMA). Small angle neutron scattering (SANS), obtained during curing, identified at least two structural phases of different length scale, for the formulations containing MF-bcP, in agreement with microstructures observed using scanning electron microscopy. Such structural electrolytes may be required when using structural electrodes that also have finer characteristic lengthscales. The addition of the MF-bcP to formulations containing 35 vol% EMIM-TFSI produced structural electrolytes with a Young's modulus of 530 MPa and an ionic conductivity of 0.64 mS cm^{-1} .

1. Introduction

Structural composite materials are increasingly used in electric vehicles, driven by the need to increase range. This rapid uptake has motivated research into composite 'structural power' storage devices. These multifunctional materials are capable of storing electrical energy, as batteries, capacitors and supercapacitors, while simultaneously carrying significant mechanical load [1–6]. Whilst a number of components require development or optimisation to achieve true multifunctionality, the electrolyte has been highlighted as one of the main challenges [6]. Electrolytes for structural energy storage devices, i.e. structural electrolytes, must have high ionic conductivity and good mechanical performance. These two properties are known [7, 8] to



have inverse relationship due to the opposite requirements, i.e. high ionic conductivity implies flexibility of the polymer chains and good mechanical properties require rigidity of these polymer chains. The inverse relationship between these two properties can be observed in the figure 1, which presents an overview of some of the best combination of the mechanical properties and ionic conductivity, presented in the literature to date.

Multifunctional materials/devices improve overall system performance by enhancing efficiencies between individual materials that provide separate functions; although the properties of the multifunctional material, in general, will be inferior to those of the monofunctional equivalents, the combined mass (or volume) may nevertheless be reduced [9]. Targets proposed in the literature [7] for structural electrolytes relevant to multifunctional energy storage devices are 1 mS cm^{-1} and 1 GPa for ionic conductivity and Young's modulus, respectively.

To date, the most promising performance has been shown by electrolytes obtained through reaction induced phase separation (RIPS). These systems have a bicontinuous structure in which one of the phases is responsible for the ion conduction while the other phase provides mechanical strength and modulus. Established systems include vinyl [2, 8, 10] and epoxy-based formulations [7, 11–13]. All these systems are initially homogeneous, but phase separate during reaction when the growing polymer chains become insoluble in the porogen/liquid electrolyte.

Epoxy-based systems are attractive for their mechanical properties, good adhesive properties and high thermal and chemical stability, as well as their widespread use in fibre composite systems. In order to introduce ionic conductivity, a range of liquid electrolytes have been explored, including ionic liquids (ILs), lithium salts, organic solvents, as well as polymers and nano-particles, both as individual compounds and in combination [7, 11, 12, 14–16].

Structural electrolytes can also be formed via RIPS using a two stage process, in which the reaction is performed in the presence of a sacrificial porogen which is then removed, and refilled with the final electrolyte [8, 17]. For example an ionic conductivity of 0.71 mS cm^{-1} was achieved by refilling the porous structure formed after removal of a low molecular weight polyethylene glycol with 1 M LiPF_6 in ethylene carbonate/diethyl carbonate [17]. In that work, the structural phase, formed using an epoxy resin with multiple oxirane rings, a block copolymer and reinforced using nano-cellulose, had a Young's modulus of 0.65 GPa . However, the manufacturing complexity of this approach makes it less applicable to real applications than single step RIPS methods ('*in situ* structural electrolytes').

The properties of RIPS-based structural electrolytes depend strongly on the composition of the initial mixture and the curing conditions. For *in situ* structural electrolytes based on epoxy formulations, ILs and their lithium salt solutions are the most widely studied liquid electrolytes/porogens [7, 11, 12, 14]. Materials with a wide range of ionic conductivities and mechanical performance have been reported depending on type and proportion of epoxy, curing agent, IL and additives [7, 8, 11, 12, 14, 18].

Bisphenol A diglycidyl ether (DGEBA) is among the extensively used epoxy resins for structural applications and has been widely studied for RIPS-based structural electrolytes, particularly in combination with 1-ethyl-3-methylimidazolium bis(fluorosulfonyl)imide (EMIM-TFSI). Using blends of DGEBA with a tetrafunctional epoxy resin resulted in a better combination of mechanical performance and ionic conductivity [11] in comparison to blends containing poly(ethylene glycol) (PEG) based epoxy resins, such as poly(ethylene glycol diglycidyl ether) (PEGDGE) [14]. Addition of PEGDGE to DGEBA resulted in an electrolyte with a maximum tensile strength of 0.8 MPa, Young's modulus <0.1 MPa, and an ionic conductivity of 0.09 mS cm^{-1} , while addition of a tetrafunctional epoxy resin led to formation of an electrolyte with Young's modulus of 480 MPa and ionic conductivity of 0.2 mS cm^{-1} . It is difficult to make a direct comparison as two different crosslinkers were used but it is reasonable to assume that the poorer performance of the electrolyte containing PEGDGE is intrinsic to the molecule; PEG is much more flexible than the aromatic DGEBA.

DGEBA based structural electrolyte formulations do not always use ILs to form an ion conducting phase. For example, lower molecular weight PEG in combination with lithium salts, such as lithium trifluoromethanesulfonate (LiTF) has also been used [15]. To counteract the plasticising effect that PEG has on epoxy, nano-silica particles were added, resulting in a structural electrolyte with ionic conductivity of 0.086 mS cm^{-1} and a tensile modulus of 135 MPa.

Whilst pure DGEBA systems are relatively simple to understand and study, the use of fully formulated commercial multicomponent epoxy resins system can offer improved performance. For example using fully formulated, commercial epoxy resin MTM57 with a solution of 2.3 M LiTFSI in EMIM-TFSI resulted in a structural electrolyte with ionic conductivity of 0.43 mS cm^{-1} and Young's modulus of 230 MPa [12].

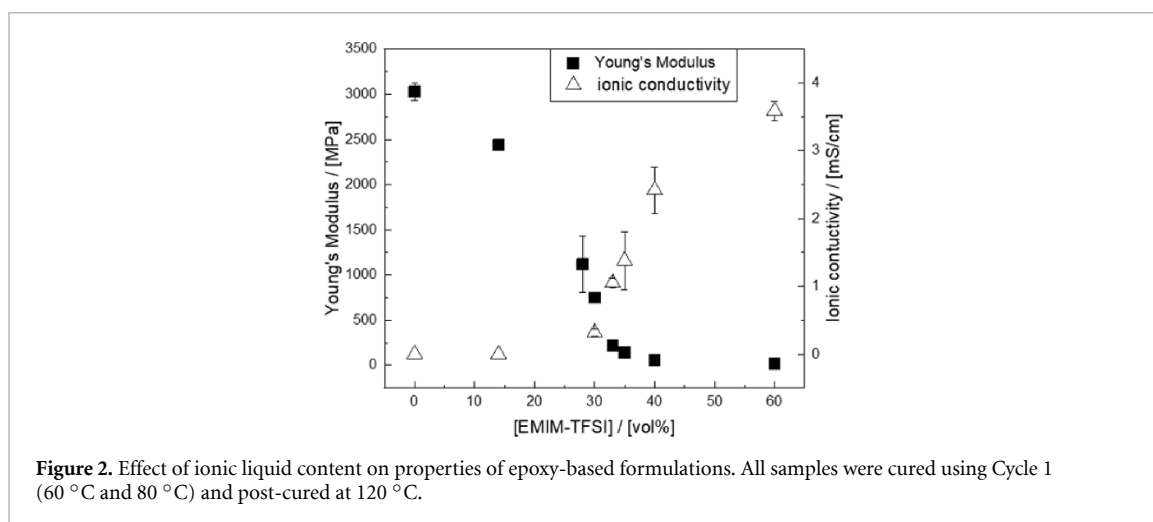
The ratio between liquid electrolyte/porogen and resin is one of the factors which dictates the balance of modulus and ionic conductivity [7, 11, 12], often through change in morphology, as well as phase proportions. Low liquid electrolyte content, i.e. just above the amount soluble in the epoxy, leads to the formation of the microstructure where droplets of the liquid electrolyte are randomly distributed in the bulk of the epoxy, resulting in samples with high mechanical performance (close to that of the neat epoxy) but negligible ionic conductivity due to the lack of a network of paths for the ion conduction [7, 11, 12]. Increasing the liquid electrolyte content leads to a change in the curing dynamics and when the proportion of liquid electrolyte becomes critical, it forms an independent, continuous phase. In this instance, the shape and scale of the structures formed by the epoxy phase plays a crucial role in the performance of the structural electrolyte. The resulting morphologies vary significantly, from fused nodules of the epoxy surrounded by the liquid electrolyte to a bicontinuous strut-like network [7, 11]. The most efficient combinations exploit a strut-like rather than fused-bead microstructure [7, 12]. The characteristic lengthscale of the microstructure is determined by the relative curing and diffusion kinetics. A coarser structure gives better modulus, but the structure must be fine enough to form a homogeneous medium around the primary structural fibres of the structural electrodes in the multifunctional composite. These structural electrodes, particularly for supercapacitors, may have a fine texture to maximise their surface area [19, 20]. In such instances, the structural electrolyte must have a characteristic lengthscale which matches the pore size of the electrode material.

To date the literature has focused on the improving the balance of mechanical properties and ionic conductivity of the bulk structural electrolyte, without considering compatibility with the electrode architecture. Here, we focus on the synthesis of a structural electrolyte with pore sizes in the submicron range and, therefore, suitable for use in combination with carbon aerogel modified carbon fibres as electrodes, with pore sizes in submicron range [19]. The lengthscale was controlled using the RIPS process by stabilising the DGEBA/IL interface, using bespoke multifunctional block-copolymers (MF-bcP). The curing kinetics of the epoxy-based formulations, with and without MF-bcP, were explored using SANS, and the resulting balance of mechanical properties and ionic conductivity discussed.

2. Results and discussion

2.1. Effect of the EMIM-TFSI concentration on the mechanical properties, ionic conductivity and morphology of the structural electrolytes

In our previous studies [12], the addition of lithium salt was essential to obtain homogeneous structural electrolytes based on blends of commercial epoxy resins and IL. Without it, macroscale/gross phase separation occurred during curing, resulting in formation of two very distinct phases, an epoxy rich top and an IL rich bottom layer. However, blends of neat DGEBA with ILs are generally reported to be stable enough to form homogeneous samples [11, 21].



In this work, the IL (EMIM-TFSI) concentration was varied in the initial formulations from 10 to 60 vol% without any evidence for macroscale/gross phase separation. The homogeneity of the samples was determined by measuring an ionic conductivity of the top and the bottom part of the samples. The formation of homogeneous samples indicated that phase separation was slower compared to the curing process. For formulations containing less than 30 vol% of EMIM-TFSI no measurable ionic conductivity was detected but the introduction of even 10 vol% led to a dramatic drop ($\sim 17\%$) in the mechanical modulus of the cured formulations (figure 2). Increasing IL content from 30 vol% to 60 vol% led to a further drop in mechanical performance but an increase in ionic conductivity (figure 2). At 60 vol%, the cured formulations became too fragile to handle, and no further increase in IL content was attempted. The observed inverse trend between mechanical performance and ionic conductivity of the formulations studied was in a good agreement with the literature [7, 8, 10, 11].

As typically observed, the modulus fell as the ionic conductivity rose, with formulations within the intermediate 30–40 vol% region presenting the best combination of properties among the formulations studied, although still relatively low. This poor trade-off is likely due to the microstructure of the structural electrolytes, since the ideal bicontinuous strut morphology was not one of the microstructures obtained (figure SI1, see supporting information, SI available online at stacks.iop.org/MFM/4/035003/mmedia).

2.2. Effect of the curing conditions on the properties and morphology of the structural electrolytes

One of the parameters influencing the morphology of the epoxy based blends is the cure temperature [22–24]. In particular, the relative rates of the cross-linking reaction and phase separation are crucial. Both processes will be affected by temperature changes [22] but, in general, to a different extent.

The curing cycle was modified to add a room temperature curing step (Cycle 2) with the expectation that the phase segregation would slow more rapidly than the curing reaction. The addition of a room temperature curing step does not have a detrimental effect on the mechanical properties of the pure DGEBA cured using isophorone diamine (iPDA) [25]. When this new cure cycle (Cycle 2) was applied to the intermediate formulations containing 33, 35 and 40 vol% of EMIM-TFSI, it led to the formation of a bicontinuous structure (figure 3) with dramatically improved performance (figure 4). Addition of the room temperature step does not only alters the shape but also the scale of the microstructural features: for example, sample IL35C1 (C1 here indicates curing Cycle 1, without a room temperature step; see section 4 for more details) had a hierarchical microstructure which consisted of at least three different types of features, similar to one reported previously [7]. The epoxy formed a continuous phase at a coarse scale (order of 100 μm) and in this phase, randomly distributed droplets of IL were observed (figures SI1(b)–(d)). The coarse, continuous epoxy phase was surrounded by connected spherical nodules (SI1(b)–(d)) with an average size of $13.9 \pm 4.1 \mu\text{m}$. The IL35 formulations cured at room temperature (Cycle 2) not only had a bicontinuous structure but the scale of the struts was almost order of magnitude smaller ($1.4 \pm 0.44 \mu\text{m}$). Similar changes in the scale of the features were observed for the other formulations studied.

As expected [26], increasing the porogen content (in this case, the IL) resulted in increased spacing between struts, (figure 3). Surprisingly, the size of structural features changed more noticeably when the EMIM-TFSI content increased from 33 to 35 vol% whilst a further increase to 40 vol% did not lead to significant changes in the size of the features.

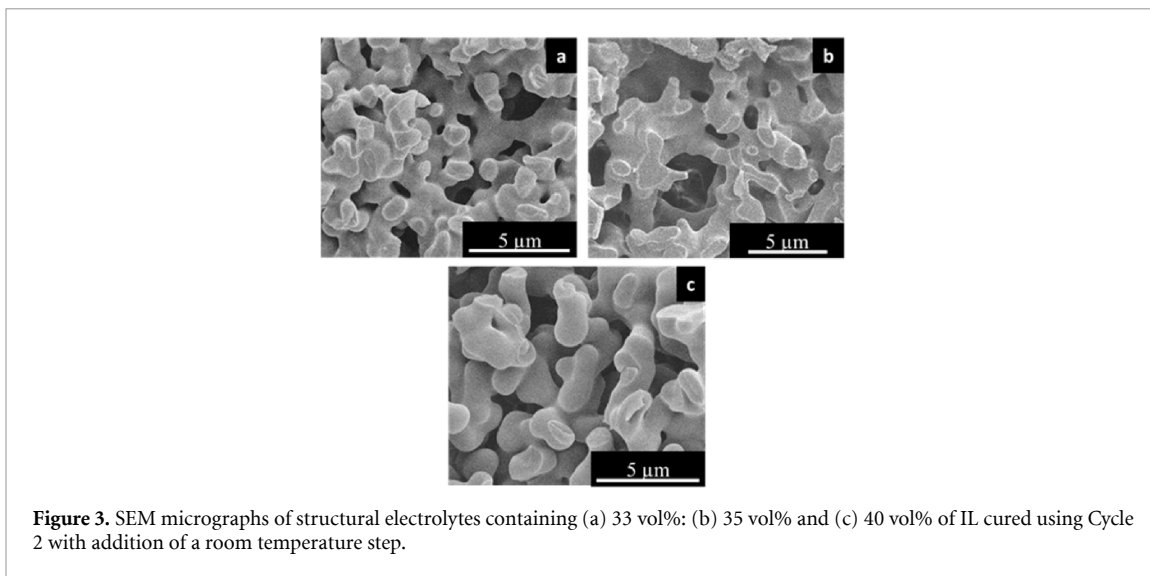


Figure 3. SEM micrographs of structural electrolytes containing (a) 33 vol%: (b) 35 vol% and (c) 40 vol% of IL cured using Cycle 2 with addition of a room temperature step.

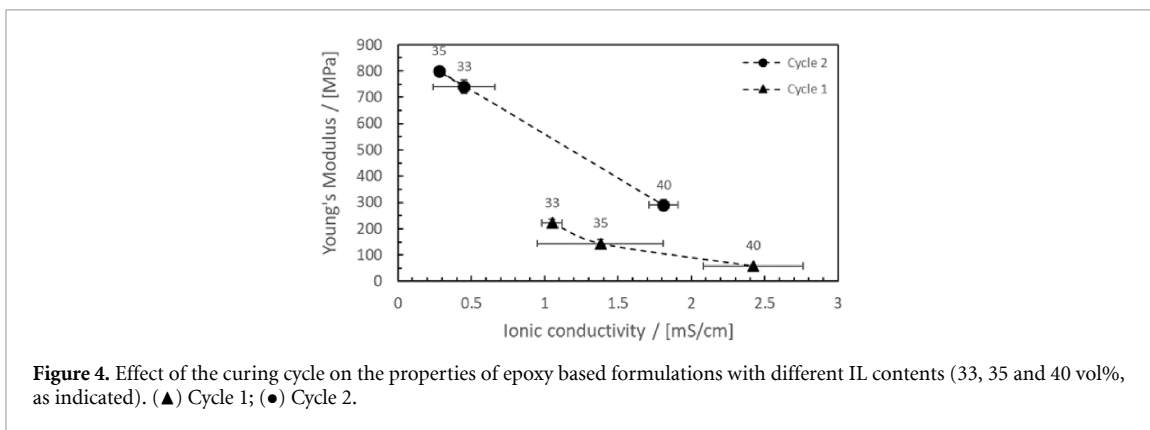


Figure 4. Effect of the curing cycle on the properties of epoxy based formulations with different IL contents (33, 35 and 40 vol%, as indicated). (▲) Cycle 1; (●) Cycle 2.

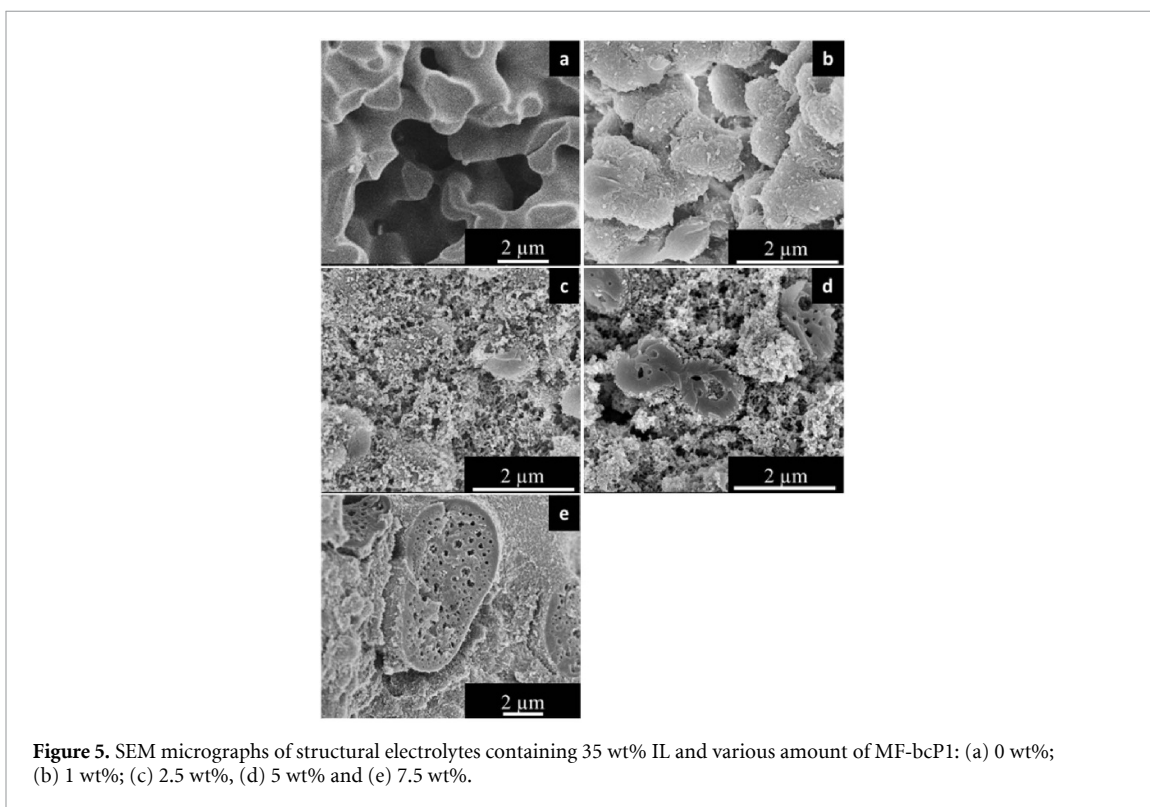


Figure 5. SEM micrographs of structural electrolytes containing 35 wt% IL and various amount of MF-bcP1: (a) 0 wt%; (b) 1 wt%; (c) 2.5 wt%, (d) 5 wt% and (e) 7.5 wt%.

Table 1. Effect of concentration of MF-bcP1 on properties of the epoxy based formulations.

Sample	IL content (vol%)	MF-bcP1 content (wt%)	Young's modulus (MPa)	Ionic conductivity (mS cm ⁻¹)
DGEBA	0	0	3030 ± 100	n.m.
IL33	33	0	740 ± 25	0.45 ± 0.21
IL33/2.5MF-bcP1	33	2.5	490 ± 20	0.15 ± 0.06
IL35	35	0	800 ± 50	0.28 ± 0.03
IL35/1MF-bcP1	35	1	200 ± 20	1.56 ± 0.09
IL35/2.5MF-bcP1	35	2.5	230 ± 13	1.35 ± 0.10
IL35/5MF-bcP1	35	5	530 ± 25	0.64 ± 0.07
IL35/7.5MF-bcP1	35	7.5	380 ± 10	0.43 ± 0.01
IL40	40	0	290 ± 20	1.81 ± 0.10
IL40/1MF-bcP1	40	1	160 ± 20	1.87 ± 0.27
IL40/2.5MF-bcP1	40	2.5	220 ± 15	1.58 ± 0.05
IL40/5MF-bcP1	40	5	60 ± 25	1.04 ± 0.05
IL40/7.5MF-bcP1	40	7.5	80 ± 7	1.10 ± 0.03

n.m.—not measurable.

These observed microstructural changes using a room temperature cure contrast with a previous report [23] that a lower curing temperature resulted in an increase in the scale of the microstructural features. In the present study, the IL acts as a diluent causing a reduction in the reactive components' concentration. Even though imidazolium is known to react with epoxy groups [27, 28], it does so at elevated temperatures. Dilution of the reaction mixture will reduce the rate of the curing process and increase mobility of the newly formed polymer chains, therefore slowing down the phase separation process.

Despite the similarity in their morphologies, the ionic conductivity and mechanical performance of the formulations are very different (figure 4), especially for the sample containing 40 vol% of IL (IL40). On closer inspection, for IL40 cured using Cycle 2 (See supporting information, figure SI2), nodular features were identified in the microstructure. These features suggest that, for this particular formulation (IL40), structural freezing took place significantly later in comparison to the other two formulations (IL33 and IL35), leading to a beginning of the struts continuity disruption due to an increase in interfacial tension [22, 29]. It is reasonable to assume that the points where nodules are connected correspond to weak points, reducing the overall mechanical performance, as shown by data reported in figure 4. However, the increase in pore size had a positive effect on the ionic conductivity.

As the combination of properties achieved was very promising, the room temperature cure was applied for all subsequent formulations.

2.3. Effect of block-copolymer on the properties of the structural electrolyte

Even though addition of the room temperature step during the cure resulted in the reduction of the scale of the microstructure, it is still too large to be compatible with many established structural electrodes, especially those used in structural supercapacitors, based on carbon aerogel (which require submicron lengthscale) [19]. Adding block-copolymers to epoxy formulations generally produces nanostructured materials [30–32]. In this study, MF-bcP, with general formulae p(GMA)_n-block-co-p(DMAEMA-TFSI)_m (scheme 1), were used to create a finer biphasic microstructure in the primary epoxy-IL system. As shown in scheme 1, one of the blocks has an oxirane ring and is compatible with DGEBA, whilst the other block contains an anion identical to that in the IL, i.e. EMIM-TFSI. It was established that p(GMA)₃₅-block-co-p(DMAEMA-TFSI)₁₇ (MF-bcP1) and p(GMA)₃₅-block-co-p(DMAEMA-TFSI)₇ (MF-bcP2) self-assemble in the presence of the EMIM-TFSI, forming micelles with diameters of 10 ± 4 nm and 23 ± 9 nm respectively, as determined by stained transmission electron microscopy (TEM) (see supporting information, figure SI3). The block-copolymers were also confirmed to self-assemble in the blends of DGEBA and EMIM-TFSI (see supporting information, figure SI4). Details of the block-copolymer synthesis can be found in the SI. The block copolymers were added in various combinations to the primary epoxy-IL system (table 1), and then cured. All samples cured using the room temperature curing cycle (Cycle 2).

The addition of MF-bcP1 to the epoxy-IL blends with EMIM-TFSI content ranging from 33 to 40 vol% led to a complex hierarchical microstructure (figures 5 and 6). Generally, the presence of the MF-bcP1 created a fine structure (in a range of 50 nm), but the longer lengthscale microstructure associated with the epoxy reverted to the fused nodule structure, and generally a reduced modulus (table 1, figure 5(b)). Where the nanostructure formed struts connecting the larger nodules (as observed for IL35), the modulus recovered (table 1, figures 5(c) and (d)) but did not achieved the performance of the original formulations without

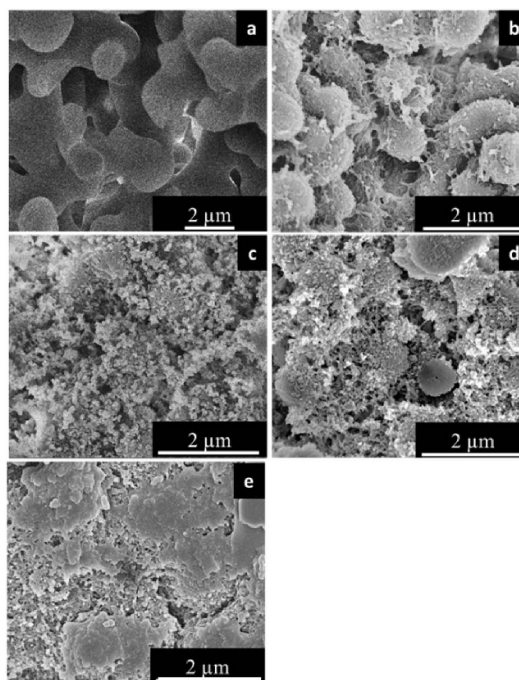


Figure 6. SEM micrographs of structural electrolytes, containing 40 wt% EMIM-TFSI and various amount of MF-bcP1: (a) 0 wt%; (b) 1 wt%; (c) 2.5 wt%, (d) 5 wt% and (e) 7.5 wt%.

Table 2. Effect of 2.5 wt% addition of different block-copolymers on the properties of the epoxy based formulations.

Sample	Block copolymer formulae	Young's modulus (MPa)	Ionic conductivity (mS cm^{-1})
IL40		290 ± 20	1.81 ± 0.10
IL40/2.5MF-bcP1	p(GMA) ₃₅ -block-co-p(DMAEMA-TFSI) ₁₇	220 ± 15	1.58 ± 0.05
IL40/2.5MF-bcP2	p(GMA) ₃₅ -block-co-p(DMAEMA-TFSI) ₇	170 ± 45	1.87 ± 0.10

^a Curing cycle 2 was used; DGEBA:iPDA molar ratio 2:1.

block-copolymer. The result is not surprising since thinner struts are less effective at withstanding mechanical load than thicker ones [33].

Differences observed in the effect of MF-bcP1 on the formulations can be attributed to the complex nature of the polymerisation of DGEBA in the presence of the IL and block-copolymers. A dramatic change in the morphology of the cured formulations was observed. As shown in figures 5 and 6, the bicontinuous structures with a strut size of $\sim 2\text{--}2.5 \mu\text{m}$ observed for cured formulations without block-copolymer transformed into rather complex structures with MF-bcP1 added. The addition of only 1 wt% to IL35 and IL40 led to the formation of platelets, in the case of IL35, and nodules for IL40, of similar dimensions with a number of fine structures connecting the platelets or nodules (figures 5(b) and 6(b)).

Since the block copolymer self-assembles in the presence of DGEBA, IL may be carried into the epoxy phase within the micelles. This effect may reduce the modulus of the larger epoxy struts and reduce the volume of the connected IL network. Conversely, it is reasonable to suppose that inverse micelles may carry epoxy into the IL phase, creating the fine nanostructures observed in figures 5(c)–(e) and 6(b)–(e). A reduction in the size of the characteristic structures in the epoxy based formulation upon addition of the block copolymer was also observed by Sakakibara *et al* [17].

As shown in table 2 and figure 7, reducing the size of the ionic block (scheme 1) did not significantly affect the microstructure or properties of the resulting structural electrolyte.

2.4. Structural changes during curing and phase separation

Changes in microstructure during curing with the addition of the MF-bcP were also studied *in situ* using small angle neutron scattering (SANS). Figure 8 shows the evolution of the SANS patterns of the IL40 sample with and without the addition of 2.5 wt% MF-bcP2. Similar to other cross-linked systems such as polymer

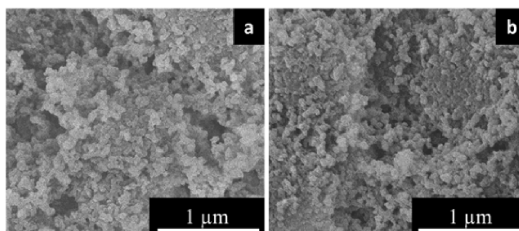


Figure 7. SEM micrographs of structural electrolytes based on epoxy formulation, containing 40 wt% EMIM-TFSI and (a) 2.5 wt% of MF-bcP1 and (b) 2.5 wt% of MF-bcP2.

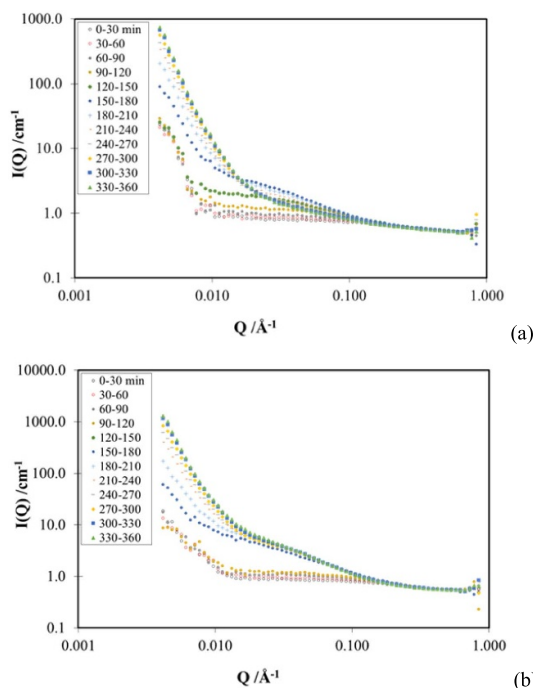


Figure 8. SANS data for IL40 (a) without and (b) with MF-bcP2, during curing. Samples consist of epoxy and iPDA in the presence of partially deuterated EMIM-TFSI (a mixture of 50:50 wt% of deuterated and non-deuterated IL was used) (time interval 30 min).

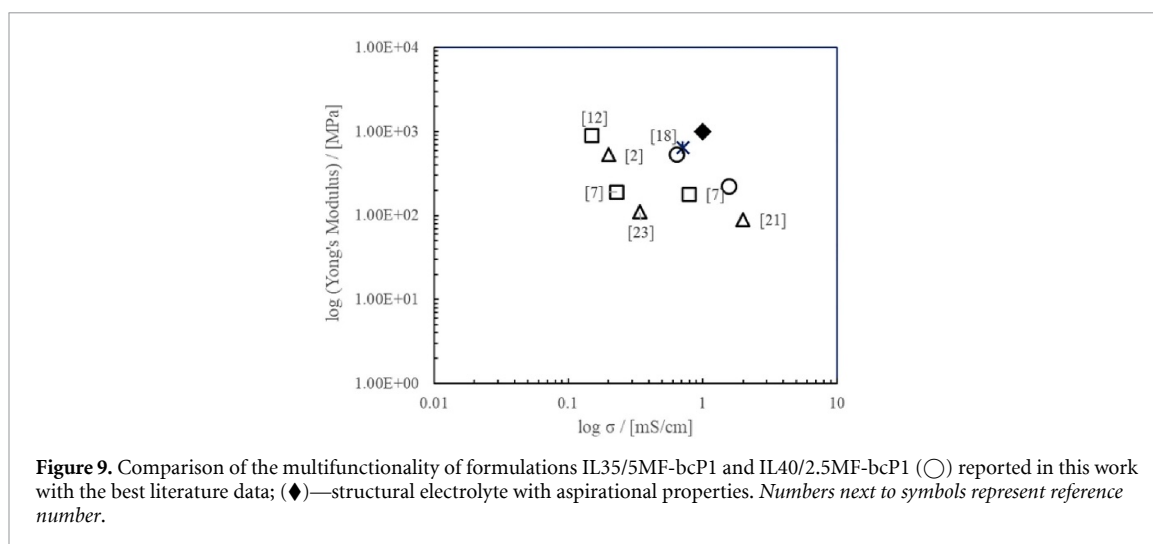
gels or thermosetting resins, the decay of the scattered intensity provides evidence for the existence of structural features at two different length scales [34]. In the first hour of the curing process, at $Q < 0.01 \text{ \AA}^{-1}$, the $I(Q)$ data display a peak whose maximum is of the order of the lowest experimentally accessible Q value (figure 8(a)). This feature could have been due to formation of self-assembled structures but measurements at lower Q are needed for confirmation.

The SANS data are consistent with models developed for cross-linked polymer gels [35–38] and later applied to thermosets [39–42]. Thus, the total scattering is given by the sum of two separate contributions:

$$I(Q)_{\text{tot}} = I(Q)_L + I(Q)_S$$

due to small structures at high Q , $I(Q)_L$, and large structures, $I(Q)_S$, at low Q . The former have been assigned to long-range static inhomogeneities whereas the latter result from local liquid-like fluctuations [34–36, 38, 43]. For IL40 without MF-bcP2 (figure 8(a)) practically no change in the size of the static inhomogeneities at $Q < 0.010 \text{ \AA}^{-1}$ were observed during the first few hours of curing, with only small variations in the extent of liquid-like fluctuations. Upon further curing, an increase in the scattered intensity at $Q < 0.1 \text{ \AA}^{-1}$ was observed. In this region, the Q dependence approximately followed Porod's law (Q^{-4} dependence), as expected for two-phase systems with large domains [44]. The shift towards higher Q with curing suggests a decrease in the characteristic length scale of the phase separated structure (figure 8(a)).

Addition of MF-bcP2 did not lead to changes in the curing kinetics during the first two hours. For longer curing time, at $Q > 0.01 \text{ \AA}^{-1}$, very little change was observed in the size of the inhomogeneities at smaller



length scale (figure 8(b)). At large length scales ($Q < 0.01 \text{ \AA}^{-1}$), the trend was analogous to that observed in absence of MF-bcP2.

2.5. Multifunctionality of the structural electrolytes

A multifunctionality plot is considered to be the best way of showing the relationship between ionic conductivity and mechanical performance of the structural electrolytes (figure 9). The position of the structural electrolyte with properties considered in the literature as ‘target properties’ [20], i.e. Young’s modulus of 1 GPa and ionic conductivity of 1 mS cm^{-1} are presented on the graph using the ‘◆’ symbol. Comparison of the best structural electrolytes reported in this paper with those reported in the literature to date showed that addition of 5 wt% of block-copolymer not only reduced the morphological feature sizes to that more compatible with CAG, but also matched the performance of those achieved through refilling of prefabricated porous membranes (figure 9). Compared to other electrolytes obtained using RIPS, the electrolytes reported in this paper showed superior performance. Further tuning of the block-copolymer composition could result in further improvement of the control of morphology and properties of the resulting structural electrolytes.

3. Conclusions

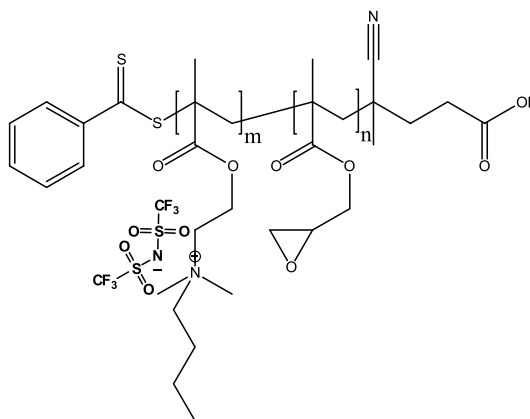
Structural electrolytes based on DGEBA were obtained using an IL as an ion provider as well as a porogen. Polymers with a wide range of microstructures and properties were obtained. The desired microstructure comprised of bicontinuous struts with submicron dimensions. Room temperature curing allowed a reduction in microstructural feature size by an order of magnitude through the suppression of the phase segregation, allowing a formation of a favourable architecture. This reduction in the lengthscale of the microstructural features resulted in a rise of the Young’s modulus and reduction of the ionic conductivity. Addition of MF-bcP resulted in formation of the hierarchical microstructure with some features in the nanometer scale. Tuning the block length of the copolymer as well as its overall molecular weight may be a fruitful area for future improvements. Effective structural electrolytes are essential for structure power composites, and simple RIPS systems offer a practical implementation.

4. Experimental

4.1. Materials

DGEBA and hardener iPDA were purchased from Sigma Aldrich. The IL, EMIM-TFSI, (>99%) was purchased from Ionic Liquid Technologies (IOLITEC, Germany). All chemicals were used as received.

The block-copolymer, poly(glycidyl methacrylate)-block-poly[(2-dimethylamino)ethyl methacrylate] butyl bis(trifluoromethane)sulfonimide] (pGMA)_n-b-p(DMAEMA-TFSI)_m, herein after referred to as (MF-bcP) was synthesised according to a method reported elsewhere [45] with $n = 35$ and m was 17 and 7 for MF-bcP1 and MF-bcP2 respectively. The detailed synthetic procedure can be found in the SI. The general structure of the MF-bcP is shown in scheme 1.



Scheme 1. General structure of the multifunctional block-copolymer (pGMA)_m-block-co-p(DMAEMA-TFSI)_n.

Table 3. Composition of the formulations studied.

Sample ^a	DGEBA (g)	iPDA (g)	EMMI-TFSI (g)	MF-bcP (g)
IL40 + 1MFbcP1	5	1.263	5.746	0.120
IL40 + 2.5MFbcP1	5	1.283	5.746	0.300
IL40 + 5MFbcP1	5	1.317	5.746	0.600
IL40 + 7.5MFbcP1	5	1.349	5.746	0.900
IL40 + 2.5MbcP2	5	1.302	5.746	0.300
IL35 + 1MFbcP1	5	1.262	4.641	0.109
IL35 + 2.5MFbcP1	5	1.280	4.641	0.272
IL35 + 5MFbcP1	5	1.310	4.641	0.545
IL35 + 7.5MbcP1	5	1.341	4.641	0.817
IL40 + 2.5MFbcP2	5	1.299	5.746	0.279

^a All calculations were done fixing amount of DGEBA to 5 g and 2:1 molar ratio of DGEBA:iPDA.

MF-bcP1—p(GMA)₃₅-block-co-p(DMAEMA-TFSI)₁₇; MF-bcP2—p(GMA)₃₅-block-co-p(DMAEMA-TFSI)₇.

4.2. Preparation of the structural electrolyte

For samples without MF-BcP, DGEBA (5 g) was mixed with EMIM-TFSI, followed by iPDA (1.25 g). The mixture was then stirred until a homogeneous solution was achieved, and was degassed under vacuum. For the samples with MF-BcP, firstly the appropriate quantity of MF-BcP was added to the DGEBA (amount of MF-bcP was calculated as wt% to the amount of IL33, IL35 and IL40 respectively), followed by addition of EMIM-TFSI (table 3). The resulting mixture was then stirred until the polymer was fully dissolved using a roller mixer (SciLogex MX-T6-S). iPDA was then added to the solution and the mixture was stirred and degassed. Prepared formulations were cured using glass moulds, with dimensions 50 mm × 80 mm × 2 mm, coated with Chemlease™ 41-90 EZ. Curing was done in a fan assisted oven (Lenton) using one of two cycles:

Cycle 1: Ramp to 60 °C at 2° min⁻¹; dwell at 60 °C for 1 h; ramp to 80 °C at 2° min⁻¹; dwell at 80 °C for 2 h=. Samples were cooled down to the room temperature following by a post-cure at 120 °C for 2 h;

Cycle 2:: Mixture was kept at room temperature for 18 h; ramp to 60 °C at 2° min⁻¹; dwell at 60 °C for 1 h; ramp to 80 °C at 2° min⁻¹; dwell at 80 °C for 2 h. Samples were cooled down to the room temperature following by a post-cure at 120 °C for 2 h.

All samples which were cured using Cycle 1 are marked as C1. All other samples were cured using Cycle 2. The composition of the studied formulations containing MF-bcP are summarised in table 3.

4.3. Neutron scattering

The SANS measurements were carried out on the SANS instrument ZOOM at ISIS facility (Rutherford Appleton Laboratory, Didcot UK). Experiments were performed *in situ* during room temperature cure. For all background samples and solutions of block-copolymers Hellma liquid cells were used. To study the curing kinetics a modified Durham cells with the thickness of 1 mm inner diameter of 10 mm, and quartz windows were used.

4.4. Characterisation of the structural electrolytes

Mechanical performance of the cured formulations was characterised using 3-point bending test at room temperature. Young's modulus was determined using the LR5KPlus advanced materials testing machine

(Lloyd Instruments/Ametek). Tests were performed on rectangular specimens with dimensions: length 24 mm, width 5 ± 0.2 mm; thickness 2 ± 0.1 mm, cut from the cured plaque. The Young's modulus was determined as

$$E_b = \frac{l^3}{4wh^3} S \quad (1)$$

where E_b is the Young's modulus (MPa), l is the sample length (mm); w is the width of the specimen (5 ± 0.2); h is the sample height (mm); S is the slope (N mm^{-1}) at the steepest ascend of the measurement. The average of a minimum of five specimens was tested for each structural electrolyte.

The ionic conductivity of the cured formulations was studied at room temperature using impedance spectroscopy on VersaSTAT 3-450 potentiostat (AMETEC) in the frequency range 10^5 –0.1 Hz with a sinusoidal voltage of amplitude 5 mV. For each formulation, two plaques of $50 \text{ mm} \times 12 \text{ mm} \times 2 \text{ mm}$ were cut from the top and bottom of the cured plaque and polished. A thin layer of EMIM-TFSI was added to the surface of the sample to minimise contact resistance and compensate for any IL removed during polishing. For each formulation, at least 10 measurements were done. The examples of the high frequency region of the Nyquist plots are presented in figures SI6 and SI7.

To study morphology EMIM-TFSI was extracted from the cured formulations as follows. A pre-weighed specimen was placed in the sample vial and ethanol was added. Ethanol was changed at least five times and specimen was subsequently dried in the vacuum oven.

The scanning electron microscopy (SEM) was performed using the FEI Helios Nanolab 600, with accelerating voltages between 3.5 kV and 10 kV. Samples after EMIM-TFSI extraction were used. Freshly fractured sample was fixed on the sample mount with conductive silver paint and sputtered with ca. 25 nm layer (thickness monitored by Cressington Thickness Monitor MTM10) of platinum (Cressington Coating System 328) or gold (Cressington Coating System 108 Auto) prior to observation under SEM. To evaluate changes in morphology, sizes of the observed features were measured using the software ImageJ.

Data availability statement

The data that support the findings of this study are available upon reasonable request from the authors.

Acknowledgments

The authors would like to acknowledge EPSRC for the financial support under the project 'Beyond structural: multifunctional composites that store electrical energy' EP/P007546/1 and Science & Technology Facilities Council ISIS for the facility access (ZOOM; experiment RB2000031 (<https://doi.org/10.5286/ISIS.E.RB2000031>)).

Conflict of interest

There are no conflicts to declare.

ORCID iD

Natasha Shirshova  <https://orcid.org/0000-0002-0546-6278>

References

- [1] Carlstedt D and Asp L E 2020 *Composites B* **186** 107822
- [2] Schneider L M, Ihrner N, Zenkert D and Johansson M 2019 *ACS Appl. Energy Mater.* **2** 4362–9
- [3] Shirshova N, Qian H, Shaffer M S P, Steinke J H G, Greenhalgh E S, Curtis P T, Kucernak A and Bismarck A 2013 *Composites A* **46** 96–107
- [4] Carlson T, Ordés D, Wysocki M and Asp L E 2010 *Compos. Sci. Technol.* **70** 1135–40
- [5] Snyder J F, Carter R H and Wetzel E D 2007 *Chem. Mater.* **19** 3793–801
- [6] Asp L E and Greenhalgh E S 2014 *Compos. Sci. Technol.* **101** 41–61
- [7] Shirshova N et al 2013 *J. Mater. Chem. A* **1** 15300–9
- [8] Gienger E B, Nguyen P-A T, Chin W, Snyder K D B J F and Wetzel E D 2015 *J. Appl. Polym. Sci.* **42** 42681
- [9] Ferreira A D B L, Nóvoa P R O and Marques A T 2016 *Compos. Struct.* **151** 3–35
- [10] Ihrner N, Johannisson W, Sieland F, Zenkert D and Johansson M 2017 *J. Mater. Chem. A* **5** 25652–9
- [11] Matsumoto K and Endo T 2008 *Macromolecules* **41** 6981–6
- [12] Shirshova N, Bismarck A, Greenhalgh E S, Johansson P, Kalinka G, Marczewski M J, Shaffer M S P and Wienrich M 2014 *J. Phys. Chem. C* **118** 28377–87
- [13] Choi U H and Jung B M 2018 *Macromol. Res.* **26** 459–65

- [14] Lim J Y, Kang D A, Kim N U, Lee J M and Kim J H 2019 *J. Membr. Sci.* **589** 117250
- [15] Feng Q, Yang J, Yu Y, Tian F, Zhang B, Feng M and Wang S 2017 *Mater. Sci. Eng. B* **219** 37–44
- [16] Li S, Jiang H, Tang T, Nie Y, Zhang Z and Zhou Q 2018 *Mater. Chem. Phys.* **205** 23–28
- [17] Sakakibara K, Kagata H, Ishizuka N, Satoc T and Tsujii Y 2017 *J. Mater. Chem. A* **5** 6866–73
- [18] Yu Y, Zhang B, Wang Y, Qi G, Tiana F, Yang J and Wang S 2016 *Mater. Des.* **104** 126–33
- [19] Qian H, Kucernak A R, Greenhalgh E S, Bismarck A and Shaffer M S P 2013 *ACS Appl. Mater. Interfaces* **5** 6113–22
- [20] Shirshova N, Qian H, Houllé M, Steinke J H G, Kucernak A R J, Fontana Q P V, Greenhalgh E S, Bismarck A and Shaffer M S P 2014 *Faraday Discuss.* **172** 1–23
- [21] Oliveira Da Silva L C and Soares B G 2018 *J. Appl. Polym. Sci.* **135** 45838
- [22] Inoue T 1995 *Prog. Polym. Sci.* **20** 119–53
- [23] Tsujioka N, Ishizuka N, Tanaka N, Kubo T and Hosoya K 2008 *J. Polym. Sci. A* **46** 3272–81
- [24] Zhang R and Zhang L 2008 *Polym. Bull.* **61** 671–7
- [25] Patel A, Kravchenko O and Manas-Zloczower I 2018 *Polymers* **10** 125
- [26] Krebs H, Yang L, Shirshova N and Steinke J H G 2012 *React. Funct. Polym.* **72** 931–8
- [27] Rahmathullah M A M, Jeyarajasingam A, Merritt B, VanLandingham M, McKnight S H and Palmese G R 2009 *Macromolecules* **42** 3219–21
- [28] Soares B G, Livi S, Duchet-Rumeau J and Gerard J-F 2011 *Macromol. Mater. Eng.* **296** 826–34
- [29] Mi Y, Zhou W, Li Q, Zhang D, Zhang R, Ma G and Su Z 2015 *RSC Adv.* **5** 55419–27
- [30] Maiez-Tribut S, Pascault J P, Soule E R, Borrajo J and Williams R J J 2007 *Macromolecules* **40** 1268–73
- [31] Yi F, Yu R, Zheng S and Li X 2011 *Polymer* **52** 5669–80
- [32] Leonardi A B, Zucchi I A and Williams R J J 2015 *Eur. Polym. J.* **65** 202–8
- [33] Chen W, Watts S, Jackson J A, Smith W L, Tortorelli D A and Spadaccini C M 2019 *Sci. Adv.* **5** eaaw1937
- [34] Shibayama M 2011 *Polym. J.* **43** 18–34
- [35] Bastide J and Leibler L 1988 *Macromolecules* **21** 2647–9
- [36] Bastide J and Candau S J 1996 *Physical Properties of Polymeric Gels* (New York: Wiley)
- [37] Berts I, Gerelli Y, Hilborn J and Rennie A R 2013 *J. Polym. Sci. B* **51** 421–9
- [38] Shibayama M, Takata S-I and Norisuye T 1998 *Physica A* **249** 245–52
- [39] Aoki M, Shundo A, Kuwahara R, Yamamoto S and Tanaka K 2018 *Macromolecules* **52** 2075–82
- [40] Izumi A, Nakao T, Iwase H and Shibayama M 2012 *Soft Matter* **8** 8438–45
- [41] Izumi A, Nakao T and Shibayama M 2013 *Soft Matter* **9** 4188–97
- [42] Izumi A, Nakao T and Shibayama M 2015 *Polymer* **59** 226–33
- [43] Shibayama M 1998 *Macromol. Chem. Phys.* **199** 1–30
- [44] Izumi A, Shudo Y, Nakao T and Shibayama M 2016 *Polymer* **103** 152–62
- [45] Wang S, Shi Q X, Ye Y S, Xue Y, Wang Y, Peng H Y, Xie X L and Mai Y W 2017 *Nano Energy* **33** 110–23